Nuclear moment of inertia as an indicator of the phase transition in a finite system

Kosai Tanabe[1,2] and Kazuko Sugawara-Tanabe[1,3]
[1]*Theoretical Nuclear Physics Laboratory, RIKEN Nishina Center, Wako, Saitama 351-0198, Japan*
[2]*Department of Physics, Saitama University, Sakura-Ku, Saitama 338-8570, Japan*
[3]*Otsuma Women's University, Tama, Tokyo 206-8540, Japan*
(Received 5 January 2015; revised manuscript received 16 February 2015; published 25 March 2015)

The purpose of this article is to derive the analytic expression for the angular-momentum dependence (I dependence) of the moment of inertia in microscopic mean-field theory for both even-even and odd-mass nuclei. Based on the constrained Hartree-Fock-Bogoliubov theory, the Coriolis antipairing effect is taken into account as the second-order perturbation to the BCS basis together with the blocking effect. Instead of integration, an asymptotic series expansion is applied to the quantity in which finiteness of the nuclear system becomes tangible in the high-spin region, where the gap parameter Δ becomes much smaller than the average single-particle level distance d. As a result, Δ keeps a small but finite value even for high-spin states, showing that there is no sharp phase transition in the nucleus. Analytic formulas are derived for the I dependence of the moment of inertia for different regions of $\Delta \geqslant d/2$ and $\Delta < d/2$.

DOI: 10.1103/PhysRevC.91.034328 PACS number(s): 21.10.Re, 21.60.Ev, 21.60.Jz, 24.10.Cn

I. INTRODUCTION

In a series of articles [1–4], we have exploited and implemented the top-on-top model with angular-momentum-dependent moments of inertia. It reproduces quite well not only the excitation energy relative to the reference, i.e., $E^* - aI(I+1)$ with $a = 0.0075$ MeV and I being the total angular momentum, but also measured $B(E2)$ and $B(M1)$ values among triaxial, strongly deformed (TSD) bands in odd-mass nuclei, i.e., Lu isotopes [5–12] and ^{167}Ta [13], and also in the odd-odd nucleus ^{164}Lu [14]. The moment of inertia (MoI) seems to keep its gradual increase, which is associated with the rotational alignment of spins, along the highly excited rotational bands far above the yrast region, e.g., TSD bands. In the top-on-top model, the evolution of the nuclear intrinsic structure caused by the decrease of the pairing gap is simulated by the gradual increase of the core MoI as functions of I.

The effect of the pairing correlation on the MoI and the functional relation of the pairing gap to the rigid-body MoI are approximately estimated by Bohr and Mottelson [15] and by Bengtsson and Helgessen [16]. The Coriolis antipairing (CAP) effect was proposed by Mottelson and Valatin [17], and the perturbation treatment for this effect has been carried out by Sano and Wakai [18] for even-even nuclei and by Sugawara [19] for odd-mass nuclei including the blocking effect. Later, the self-consistent calculation based on the constrained Hartree-Fock-Bogoliubov (CHFB) equation showed that the phase transition from the superconducting state with a finite gap value Δ ($\neq 0$) to the normal state with $\Delta = 0$ occurs stepwise starting from the decrease of the gap in the unique-parity high-j level (gapless superconductor) [20].

An attempt has been made to simulate the centrifugal stretching effect in terms of the β vibration within the framework of a confined β-soft rotor model [21]. Such a model stands in sharp contrast with the self-consistent solution to the CHFB equation, which describes automatically the centrifugal stretching effect as well as the effect arising from the pairing interaction. The CHFB solutions have shown that the CAP effect plays a much more important role in the evolution of the nuclear structure along the ground bands than the centrifugal stretching effect. Some examples of the CHFB result taking into account the pairing interaction and the quadrupole-quadrupole interaction are shown in Ref. [22].

It has been argued that the projection of the particle number [23] and/or the projection of the angular momentum [24] prevents the rapid decrease of Δ and keeps its finite value even in high-spin states. In these methods, Δ is deduced from the expectation value of the pairing interaction. However, the original concept of the gap is an order parameter defined in terms of the quasivacuum expectation value of the product of two annihilation (or creation) single-particle operators. In this article, bearing in mind such a problem, we derive analytic formulas of the functional dependence of the MoI and the gap on I from the mean-field theory.

In Sec. II, we begin with the CHFB equation and treat the cranking term as perturbation for the even-even nucleus with axially symmetric deformation. In Sec. III, we provide an analytic integral for the MoI formula by an approximation similar to the one adopted in Refs. [15,16]. In Sec. IV, applying the same approximation method as used in Sec. III, we relate I to the gap Δ ("integral form"). In Sec. V, we propose a method to perform summation consistent with the finiteness of the nuclear system, wherein Δ is much smaller than the level distance d ("sum form"). In Sec. VI, our formalism is extended to the odd-mass nucleus. In Sec. VII, we compare the MoI between even-even and odd-mass cases in both the integral form and the sum form. In Sec. VIII, the article is concluded. Some relevant mathematical operations are summarized in Appendices A, b, and C.

II. PERTURBATION SOLUTION TO CHFB EQUATION IN EVEN-EVEN NUCLEUS

We consider the case of an axial-symmetrically deformed even-even nucleus. To develop our discussion as transparently as possible, we take into account only the pairing interaction because the effect of the other interactions is assumed to be

included in the single-particle energy. The CHFB Hamiltonian is given by

$$\begin{aligned} H &= H_0 - H_\Omega, \\ H_0 &= \sum_\alpha (\varepsilon_\alpha - \lambda) c_\alpha^\dagger c_\alpha - \frac{G}{4} \sum_{\alpha,\beta} c_{\tilde{\alpha}}^\dagger c_\alpha^\dagger c_\beta c_{\tilde{\beta}}, \\ H_\Omega &= \Omega_x \hat{I}_x, \quad \text{with} \quad \hat{I}_x = \sum_{\alpha,\beta} (j_x)_{\alpha\beta} c_\alpha^\dagger c_\beta, \end{aligned} \tag{1}$$

where ε_α is the single-particle energy in the deformed field; λ the chemical potential, which is determined from the constraint on the particle-number; G the pairing strength; and Ω_x the Lagrange multiplier (or rotational frequency about the x axis), which is determined from the constraint on the total angular-momentum operator $\hat{I}_x$. The particle operators describing the single-particle states in the axial-symmetrically deformed field are represented by $\{c_\alpha^\dagger, c_\alpha\}$ and their time-reversed ones $\{c_{\tilde{\alpha}}^\dagger, c_{\tilde{\alpha}}\}$.

The quasiparticle operators $\{\alpha_i^\dagger, \alpha_i\}$ are introduced through the Bogoliubov transformation:

$$\alpha_i^\dagger = \sum_\alpha (A_{i\alpha} c_\alpha^\dagger + B_{i\alpha} c_\alpha). \tag{2}$$

We have orthonormality relations as a part of the unitarity nature of this transformation:

$$\begin{aligned} &\sum_\alpha (A_{i\alpha}^* A_{j\alpha} + B_{i\alpha}^* B_{j\alpha}) = \delta_{ij}, \\ &\sum_\alpha (A_{i\alpha} B_{j\alpha} + B_{i\alpha} A_{j\alpha}) = 0, \\ &\sum_i (A_{i\alpha} A_{i\beta}^* + B_{i\alpha}^* B_{i\beta}) = \delta_{\alpha\beta}, \\ &\sum_i (A_{i\alpha} B_{i\beta}^* + B_{i\alpha}^* A_{i\beta}) = 0. \end{aligned} \tag{3}$$

The CHFB equations are derived through the minimization of the expectation value of H by the quasivacuum for α_i under the constraint of the first relation in Eq. (3), i.e., $\delta[\langle H \rangle + \frac{1}{2} \sum_i \Lambda_i \sum_\alpha (A_{i\alpha}^* A_{i\alpha} + B_{i\alpha}^* B_{i\alpha})] = 0$, where Λ_i is introduced as a Lagrange multiplier. Making use of the other relations in Eq. (3), we get a set of CHFB equations:

$$\begin{aligned} \Lambda_i A_{i\alpha} &= \sum_\beta [(\varepsilon_\alpha - \lambda)\delta_{\alpha\beta} - \Omega_x (j_x)_{\alpha\beta}] A_{i\beta} + \delta_{\alpha\tilde{\beta}} \Delta B_{i\beta}, \\ -\Lambda_i B_{i\alpha} &= \sum_\beta [(\varepsilon_\alpha - \lambda)\delta_{\alpha\beta} - \Omega_x (j_x)_{\alpha\beta}] B_{i\beta} + \delta_{\alpha\tilde{\beta}} \Delta^* A_{i\beta}, \end{aligned} \tag{4}$$

where the pairing gap Δ is defined by

$$\Delta = \frac{G}{2} \sum_\alpha \langle c_{\tilde{\alpha}} c_\alpha \rangle = \frac{G}{2} \sum_{i\alpha} A_{i\tilde{\alpha}} B_{i\alpha}^*. \tag{5}$$

We have neglected the contribution from the pairing interaction to the self-energy in Eq. (4).

In solving a set of the CHFB equations in Eq. (4), we deal with the cranking term H_Ω as perturbation to the BCS solution. The zeroth-order solution to Eq. (4) is given by the BCS solution, which is obtained from Eq. (4) by setting $\Omega_x = 0$, $A_{i\alpha} = \delta_{i\alpha} u_\alpha$, $B_{i\alpha} = \delta_{i\tilde{\alpha}} v_\alpha$, and $\Lambda_i = \delta_{i\alpha} E_\alpha (= \delta_{i\alpha} \sqrt{(\varepsilon_\alpha - \lambda)^2 + \Delta^2})$. The gap equation in Eq. (5) is reduced to

$$\begin{aligned} \Delta &= \frac{G}{2} \sum_\alpha u_\alpha v_\alpha, \\ u_\alpha^2 &= \frac{1}{2}\left(1 + \frac{\varepsilon_\alpha - \lambda}{E_\alpha}\right), \quad v_\alpha^2 = \frac{1}{2}\left(1 - \frac{\varepsilon_\alpha - \lambda}{E_\alpha}\right). \end{aligned} \tag{6}$$

Within a framework of the stationary perturbation theory for a nondegenerate case, we get the first-order and second-order perturbation solutions and put them into Eq. (5) together with the zeroth-order expressions given by Eq. (6). Then, up to the second-order perturbation, the gap equation becomes

$$\Delta = \frac{G}{4} \sum_\alpha \frac{\Delta}{E_\alpha} \left[1 - \Omega_x^2 \sum_\beta \frac{(j_x)_{\alpha\beta}^2}{E_\alpha + E_\beta} \left(\frac{E_\alpha E_\beta - (\varepsilon_\alpha - \lambda)(\varepsilon_\beta - \lambda) - \Delta^2}{E_\alpha E_\beta (E_\alpha + E_\beta)} + \frac{(\varepsilon_\alpha - \lambda)(\varepsilon_\alpha - \varepsilon_\beta)}{E_\alpha^2 E_\beta} \right) \right]. \tag{7}$$

This equation can be regarded as a self-consistent equation to determine Δ under the influence of the rotational effect [17–19]. In Sec. IV, applicability of the original perturbation treatment is checked numerically with a compact expression in Eq. (24).

The MoI is introduced through the constraint for the expectation value of $\hat{I}_x$ by the quasivacuum:

$$\langle \hat{I}_x \rangle = I = \mathcal{J}_x \Omega_x. \tag{8}$$

Up to the first-order perturbation, the MoI about the x axis is given by

$$\mathcal{J}_x = \sum_{\alpha,\beta\,(\varepsilon_\alpha < \varepsilon_\beta)} \frac{(j_x)_{\alpha\beta}^2}{E_\alpha + E_\beta} \left(1 - \frac{(\varepsilon_\alpha - \lambda)(\varepsilon_\beta - \lambda) + \Delta^2}{E_\alpha E_\beta} \right). \tag{9}$$

Here, we mark that the second-order perturbation does not contribute to Eq. (8) for the even-even case. The appearance of Eq. (9) is the same as the cranking formula [25,26], but Δ and λ deviate from the conventional BCS solution. We discuss the rotational effect on λ in Sec. IV.

III. GAP DEPENDENCE OF MOMENT OF INERTIA

In Refs. [15,16], under the assumption that only large matrix elements of j_x that appear in the sum of Eq. (9) contribute to $\mathcal{J}_x$ with a common excitation energy of δ ($= \varepsilon_\beta - \varepsilon_\alpha$), an analytic formula for $\mathcal{J}_x$ has been derived as a function of $\mathcal{J}_x^{\text{rig}}$ and Δ. Here, the value of δ is given by $\hbar(\omega_y - \omega_z)$ [15], with ω_y and ω_z being the harmonic oscillator strengths along the y axis and the

z axis. For a nucleus with $A = 160$ and deformation parameter $\beta \sim 0.3$, δ becomes $\sim$2.3 MeV. However, δ is the energy distance between two levels connected by j_x, and its magnitude is actually shown to be 1.4–1.5 MeV for $i_{13/2}$ levels around $\beta \sim 0.3$ [27], which is less than 2.3 MeV. In the proton shell, the average of δ for $h_{11/2}$, $g_{7/2}$, $2d_{5/2}$, $2d_{3/2}$, and $i_{13/2}$ levels is 2.1 MeV around $\beta \sim 0.3$ [27]. In what follows, choosing $\delta = 2.0$ MeV we carry out systematic analysis and display the results in the figures. All the quantities are expressed as functions of a dimensionless parameter:

$$\xi = \frac{2\Delta}{\delta}. \tag{10}$$

Note that this variable ξ is related to x in Refs. [15,16] by $\xi = 1/x$. Based on the approximation method adopted in Refs. [15,16], the quantity under the sum in Eq. (9) is replaced by the product of two factors:

$$\mathcal{J}_x \cong \sum_{\alpha,\beta\,(\varepsilon_\alpha<\varepsilon_\beta)} (j_x)^2_{\alpha\beta} \left\langle \frac{E_\alpha E_\beta - (\varepsilon_\alpha - \lambda)(\varepsilon_\beta - \lambda) - \Delta^2}{(E_\alpha + E_\beta)E_\alpha E_\beta} \right\rangle_{\rm av}$$
$$\equiv 2 \sum_{\alpha,\beta\,(\varepsilon_\alpha<\varepsilon_\beta)} \frac{(j_x)^2_{\alpha\beta}}{\delta} \langle g \rangle_{\rm av}, \tag{11}$$

where $\langle\,\rangle_{\rm av}$ denotes an averaged value of the function within the relevant range of ε_α. Because $\varepsilon_\beta - \varepsilon_\alpha = \delta$, the sum of the first factor $(j_x)^2_{\alpha\beta}/\delta$ in Eq. (11) gives the expression for the rigid-body MoI $\mathcal{J}_x^{\rm rig}$ [25]:

$$\mathcal{J}_x^{\rm rig} = 2 \sum_{\alpha,\beta(\varepsilon_\alpha<\varepsilon_\beta)} \frac{(j_x)^2_{\alpha\beta}}{\varepsilon_\beta - \varepsilon_\alpha} \cong 2 \sum_{\alpha(\varepsilon_\beta=\varepsilon_\alpha+\delta)} \frac{(j_x)^2_{\alpha\beta}}{\delta}. \tag{12}$$

Hence, Eq. (11) becomes

$$\mathcal{J}_x = \mathcal{J}_x^{\rm rig} \langle g \rangle_{\rm av}. \tag{13}$$

The function $g(x)$ inside the bracket in Eq. (11) is expressed in terms of $x = \varepsilon_\alpha - \lambda$ as

$$g(x) = \frac{\delta}{2(\sqrt{x^2+\Delta^2} + \sqrt{(x+\delta)^2+\Delta^2})} \times \left(1 - \frac{x(x+\delta)+\Delta^2}{\sqrt{x^2+\Delta^2}\sqrt{(x+\delta)^2+\Delta^2}}\right). \tag{14}$$

In estimating the averaged value of $g(x)$, Refs. [15,16] assume $g(x)$ is sharply peaked around $\varepsilon_\alpha = \lambda - \delta/2$ in the interval $\varepsilon_{\rm min} \leqslant \varepsilon_\alpha \leqslant \varepsilon_{\rm max}$. This interval $\varepsilon_{\rm max} - \varepsilon_{\rm min}$ is expressed as δ. In Fig. 1, actual behavior of the function $g(x)$ vs x/δ is shown for $\xi = 0.2$. Note that the function is symmetric with respect to $x = -\delta/2$, and it takes finite value within a limited range of the width δ, i.e., $-\delta \leqslant x \leqslant 0$. To obtain an analytic expression for $\langle g \rangle_{\rm av}$, we consider a suitable approximation method in Appendix A. From Eq. (A3) an average value of the integrand $g(x)$ becomes

$$\langle g \rangle_{\rm av} = \frac{2}{\rho\delta} \int_{-\delta/2}^{0} \rho[g(x) + g(x-\delta)]dx$$
$$= 1 - \xi^2 \ln\left(\frac{1+\sqrt{1+\xi^2}}{\xi}\right) + \frac{19}{90}\xi^2, \tag{15}$$

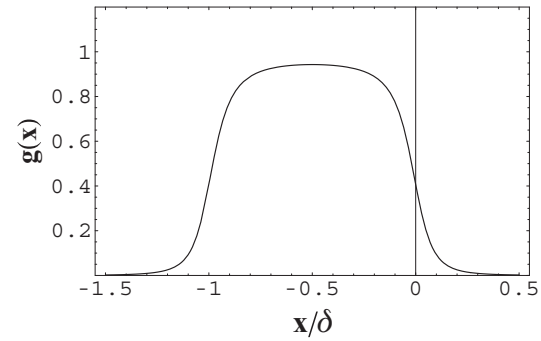

FIG. 1. Behavior of $g(x)$ in Eq. (14) as a function of $x(= \varepsilon_\alpha - \lambda)$ for $\xi(= 2\Delta/\delta) = 0.2$.

where ρ is the single-particle level density given by $1/d$ with d being the average spacing between doubly degenerate single-particle levels.

In Ref. [15], the average of $g(x)$ is calculated from the integral over the extended region from $-\infty$ to ∞ divided by the finite interval δ:

$$\langle g \rangle_{\rm av} = \frac{1}{\rho\delta} \int_{-\infty}^{\infty} \rho g(x) dx$$
$$= 1 - \frac{\xi^2}{\sqrt{1+\xi^2}} \ln\left(\frac{1+\sqrt{1+\xi^2}}{\xi}\right). \tag{16}$$

Except for $19\xi^2/90$, Eq. (15) coincides with Eq. (16), if higher orders in ξ^2 are neglected. In Ref. [16] the integral is approximated by an area of the triangle with its height of $g(x = -\delta/2)$ and its base of 2δ:

$$\langle g \rangle_{\rm av} = \frac{1}{(1+\xi^2)^{3/2}}. \tag{17}$$

According to three alternative estimates, $\langle g \rangle_{\rm av}$ is given by Eq. (15), (16), or (17). In Fig. 2, we compare $\mathcal{J}_x$ as functions of ξ $(0 \leqslant \xi \leqslant 0.8)$ calculated for three cases with $\mathcal{J}_x^{\rm rig} = 68$ MeV^{-1}. The upper dotted line labeled "BH" represents Eq. (17), the lower dashed line labeled "BM" Eq. (16), and the

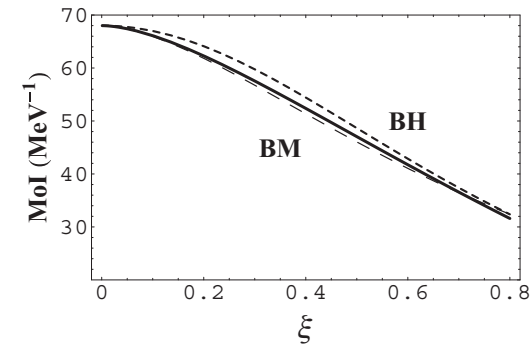

FIG. 2. Comparison of the MoI as functions of ξ for three cases with different $\langle g \rangle_{\rm av}$ and a common $\mathcal{J}_x^{\rm rig} = 68$ MeV^{-1}. Equation (17) is represented by BH (dotted line), Eq. (16) by BM (dashed line), and Eq. (15) by the solid line in the middle of BH and BM.

middle solid line Eq. (15). The three lines well overlap each other.

IV. THE I DEPENDENCE OF THE PAIRING GAP IN AN EVEN-EVEN NUCLEUS (INTEGRAL FORM)

To deal with Eq. (7) analytically, we adapt the same technique as used in deriving Eq. (15). At first we rewrite Eq. (7) in a symmetric form so as to limit the sums over the states α and β to the region of $\varepsilon_\alpha < \varepsilon_\beta$, and we introduce a common excitation energy $\delta = \varepsilon_\beta - \varepsilon_\alpha$ as in the previous section. The nontrivial solution of Δ obeys the following equation [18,19]:

$$\frac{4}{G} = \sum_\alpha \frac{1}{E_\alpha} - \Omega_x^2 \sum_{\alpha,\beta\,(\varepsilon_\alpha<\varepsilon_\beta)} (j_x)^2_{\alpha\beta} \times \left[\frac{E_\alpha E_\beta - (\varepsilon_\alpha-\lambda)(\varepsilon_\beta-\lambda) - \Delta^2}{E_\alpha^2 E_\beta^2 (E_\alpha+E_\beta)} + \delta^2 \frac{\Delta^2 - (\varepsilon_\alpha-\lambda)(\varepsilon_\beta-\lambda)}{(E_\alpha+E_\beta)E_\alpha^3 E_\beta^3} \right], \tag{18}$$

where E_β contains $\varepsilon_\beta = \varepsilon_\alpha + \delta$. The first term in the right-hand side of Eq. (18) is estimated as [28]

$$\sum_\alpha \frac{1}{E_\alpha} \cong \int_{-S/2}^{S/2} \frac{2\rho dx}{\sqrt{x^2+\Delta^2}} = 4\rho \sinh^{-1}\left(\frac{S}{2\Delta}\right), \tag{19}$$

where $\pm S/2$ are the cutoff energies. A factor 2 before ρ in the integral comes from the degeneracy of E_α and $E_{\tilde{\alpha}}$. Similarly to in Sec. III, the second term in Eq. (18) is estimated as the product of $(j_x)^2_{\alpha\beta}$ and the averaged value of the rest. Because ε_β takes the limited value $\varepsilon_\alpha + \delta$, the double sum is reduced to a single sum over ε_α. Thus, we replace the quantity in the square bracket, i.e., $[\cdots]$ in Eq. (18), with its average value:

$$\Omega_x^2 \sum_{\alpha\,(\varepsilon_\beta=\varepsilon_\alpha+\delta)} (j_x)^2_{\alpha\beta} \frac{1}{\delta} \int_{-3\delta/2}^{\delta/2} f(x)dx. \tag{20}$$

The integrand $f(x)$ is given by

$$f(x) = \frac{1}{(E_x + E_{x+\delta})E_x E_{x+\delta}} \times \left[1 - \frac{x(x+\delta)+\Delta^2}{E_x E_{x+\delta}} + \delta^2 \frac{\Delta^2 - x(x+\delta)}{(E_x E_{x+\delta})^2} \right], \tag{21}$$

where $E_x = \sqrt{x^2+\Delta^2}$ and $E_{x+\delta} = \sqrt{(x+\delta)^2+\Delta^2}$. In Fig. 3 we show the behavior of $f(x)$ for $\Delta = 0.1$ MeV and $\delta = 1$ MeV, which is symmetric with respect to $x = -\delta/2$ and has a meaningful nonzero value within the limited region $-3\delta/2 \leqslant x \leqslant \delta/2$.

Analytic integration for an approximated $f(x)$ is performed in Appendix B. Using the quantity $\bar{F}$ in Eq. (B3) together with Eqs. (19) and (12), we rewrite Eq. (18) as

$$\frac{1}{G\rho} = \sinh^{-1}\left(\frac{S}{2\Delta}\right) - \Omega_x^2 \frac{\mathcal{J}_x^{\rm rig}}{8\delta^2\rho} \bar{F}, \tag{22}$$

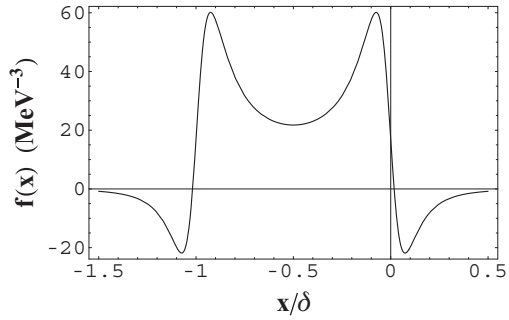

FIG. 3. Behavior of $f(x)$ in Eq. (21) as a function of $x(=\varepsilon_\alpha - \lambda)$ with $\Delta = 0.1$ MeV and $\delta = 1$ MeV.

where

$$\bar{F} = 16(1-\xi^2)\ln\left(\frac{1+\sqrt{1+\xi^2}}{\xi}\right) + \frac{319}{27}\xi^2 - \frac{371}{45}. \tag{23}$$

Now, making use of Eq. (8) for $\Omega_x = I/\mathcal{J}_x$ and Eq. (13), we rewrite Eq. (22) up to the second order in ξ as

$$\frac{\Delta}{S} \sim e^{-z}, \quad \text{with} \quad z = \frac{1}{G\rho} + \frac{I^2\bar{F}}{8\delta^2\rho\mathcal{J}_x^{\rm rig}\langle g\rangle^2_{\rm av}}. \tag{24}$$

We introduce Δ_0, which is the gap value at $I = 0$ ($\Omega_x = 0$), and define $\xi_0 \equiv 2\Delta_0/\delta = (2S/\delta)\exp[-1/(G\rho)]$ wherein parameters S and G are included. Note that the existence of many single-particle levels are in principle taken into account through ξ_0. This stands in contrast to the cases of numerical analysis with a limited number of single-particle levels [18,19]. Comparing the last term in Eq. (24) at $\xi = \xi_0$ with $1/(G\rho)$ for $G = 0.14$ MeV [28], we find that applicability of the original perturbation expansion is limited to $I < 25$.

We express Eq. (24) in an alternative form:

$$\xi = \xi_0 \exp\left[-\frac{I^2}{8\delta^2\rho\mathcal{J}_x^{\rm rig}} \left(\frac{\bar{F}}{\langle g\rangle^2_{\rm av}}\right)\right]. \tag{25}$$

Introducing a band-head angular momentum I_0, and replacing I by $I - I_0$, we solve Eq. (25) with respect to $I - I_0$ as a function of ξ:

$$I - I_0 = \left[8\delta^2\rho\mathcal{J}_x^{\rm rig} \frac{\ln(\xi_0/\xi)\langle g\rangle^2_{\rm av}}{\bar{F}} \right]^{1/2}. \tag{26}$$

In this equation, we carry out the definite integral for both $\langle g\rangle_{\rm av}$ in Eq. (15) and $\bar{F}$ in Eq. (23). We refer to both Eqs. (15) and (26) as the "integral form." This solution is illustrated in Fig. 4 with the following parameter set: $\rho = 2.5$ MeV^{-1}, $\mathcal{J}_x^{\rm rig} = 68$ MeV^{-1}, $\delta = 2.0$ MeV, and $\xi_0 = 0.8$. Figure 4 shows that ξ vanishes at the critical angular momentum of $I_c - I_0 \sim 18$. Even if the other expression for $\langle g\rangle_{\rm av}$ like in Eq. (16) or Eq. (17) is adopted, a similar result is obtained, because the behaviors of three kinds of MoI are quite similar as shown in Fig. 2.

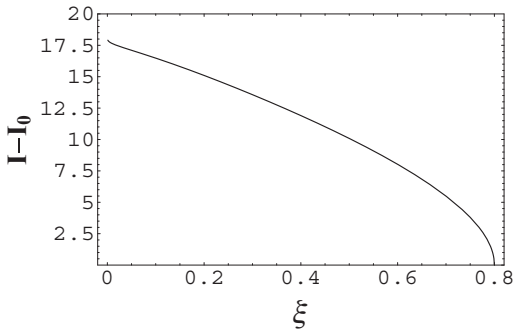

FIG. 4. The angular momentum I measured from band head I_0 calculated from Eq. (26) as a function of $\xi(=2\Delta/\delta)$. The parameters are given in the text.

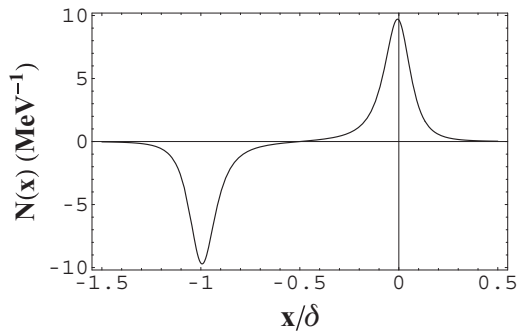

FIG. 5. Behavior of $N(x)$ in Eq. (28) as a function of $x(=\varepsilon_\alpha-\lambda)$ with $\Delta=0.1$ MeV and $\delta=1$ MeV.

Another constraint is required for the particle number N up to the second-order perturbation:

$$N=\sum_\alpha v_\alpha^2+\frac{\Omega_x^2}{2}\sum_{\alpha,\beta}\frac{(j_x)^2_{\alpha\beta}}{E_\alpha+E_\beta}\left[\frac{\varepsilon_\alpha-\lambda}{E_\alpha(E_\alpha+E_\beta)}\times\left(1-\frac{(\varepsilon_\alpha-\lambda)(\varepsilon_\beta-\lambda)+\Delta^2}{E_\alpha E_\beta}\right)-\frac{\Delta^2(\varepsilon_\alpha-\varepsilon_\beta)}{E_\alpha^3E_\beta}\right]. \tag{27}$$

The second term in Eq. (27) is rewritten in a symmetric form so as to limit the sum over states α and β to the region of $\varepsilon_\alpha<\varepsilon_\beta=\varepsilon_\alpha+\delta$. Then, Eq. (27) becomes

$$N=\sum_\alpha v_\alpha^2+\frac{\Omega_x^2}{2}\sum_{\alpha<\beta(\varepsilon_\beta=\varepsilon_\alpha+\delta)}\frac{(j_x)^2_{\alpha\beta}}{\delta}N(x),$$

with

$$N(x)=\frac{\delta}{(E_x+E_{x+\delta})^2}\left(1-\frac{x(x+\delta)+\Delta^2}{E_xE_{x+\delta}}\right)\left(\frac{x}{E_x}+\frac{x+\delta}{E_{x+\delta}}\right)+\frac{\Delta^2\delta^2}{(E_x+E_{x+\delta})E_xE_{x+\delta}}\left(\frac{1}{E_x^2}-\frac{1}{E_{x+\delta}^2}\right). \tag{28}$$

Here, E_x and $E_{x+\delta}$ are the same as defined in Eq. (21). If we apply the same approximation as used in Eq. (18), $N(x)$ becomes an odd function of $\varepsilon_\alpha-\lambda+\delta/2$. In Fig. 5, we show the behavior of $N(x)$ as a function of $x=\varepsilon_\alpha-\lambda$. It is well understood that the cancellation occurs when the sum is carried out in Eq. (28). Therefore, we expect the rotational effect on λ is small and do not take into account such an effect in the present article.

V. THE I DEPENDENCE OF Δ AND $\mathcal{J}_x$ IN THE RANGE OF $\Delta\ll 1/\rho$ (SUM FORM)

In our treatment of the gap equation, the sum over the relevant single-particle states is replaced with an integral over a certain finite range. While our approximation is excellent when Δ or ξ $(=2\Delta/\delta)$ is finite, its accuracy is not enough for small Δ, because the factor $1/E_x=1/\sqrt{x^2+\Delta^2}$ or $1/E_{x+\delta}=1/\sqrt{(x+\delta)^2+\Delta^2}$ in the right-hand side of Eq. (21) diverges at $x=0$ or $x=-\delta$, when $\Delta=0$. This fact is inferred also from the behavior of $f(x)$ at $x/\delta=0$ and -1 in Fig. 3. Therefore, we cannot carry out integration over x for the gap equation, but have to consider another approximation for the case where Δ is much smaller than the level distance d. For a nucleus with $A=160$ and the deformation parameter $\beta\sim0.3$, the average level distance d is almost 0.4 MeV, which corresponds to $\rho\equiv1/d\sim2.5$ MeV^{-1}. Finiteness of the nuclear radius or of the nuclear system reflects on the finiteness of d.

When $\Delta\ll d$, the summation must be directly carried out. We adopt the picket-fence approximation, wherein the single-particle levels are distributed symmetrically with a common level distance d in both sides of the chemical potential λ. Assuming that there are n levels within the interval $0<x\leqslant\delta/2$, we expand the relevant expression with respect to $(2\Delta/d)^2$ as follows:

$$\sum_{x>0}^{\delta/2}\frac{1}{\sqrt{x^2+\Delta^2}}\equiv\sum_{i=1}^{n}\frac{1}{\sqrt{\left(\frac{d(2i-1)}{2}\right)^2+\Delta^2}}=\frac{2}{d}\sum_{i=1}^{n}\frac{1}{2i-1}\left\{1-\frac{1}{2}\left(\frac{2\Delta}{d(2i-1)}\right)^2+\frac{3}{8}\left(\frac{2\Delta}{d(2i-1)}\right)^4+\cdots\right\}, \tag{29}$$

$$\text{with}\quad n\equiv\left[\frac{\delta+d}{2d}\right],$$

where [ ] denotes Gauss symbol. We consider the practice of the above summation in Appendix C.

According to Eq. (C6) in Appendix C, when Δ is much smaller than $d/2$, the quantity $\ln[(1+\sqrt{1+\xi^2})/\xi]$ in Eq. (15), which arises from the definite integral $\int_{-\delta/2}^{0} dx/\sqrt{x^2+\Delta^2}$, should be replaced by $\Gamma_n - \xi^2 Z_n$. Then $\langle g\rangle_{\rm av}$ should be approximated by

$$\langle g\rangle_{\rm av} \to \langle g\rangle_n \equiv 1 - \xi^2\left(\Gamma_n - \xi^2 Z_n - \frac{19}{90}\right). \quad (30)$$

Similarly, $\bar{F}$ in Eq. (23) should be replaced by

$$\bar{F} \to \bar{F}_n \equiv 16(1-\xi^2)(\Gamma_n - \xi^2 Z_n) + \tfrac{319}{27}\xi^2 - \tfrac{371}{45}. \quad (31)$$

We name both $\langle g\rangle_n$ in Eq. (30) and $\bar{F}_n$ in Eq. (31) as the "sum form." Thus, for $\Delta \ll d/2$, we have

$$I - I_0 = \left[8\delta^2\rho\mathcal{J}_x^{\rm rig}\frac{\ln(\xi_0/\xi)\langle g\rangle_n^2}{\bar{F}_n}\right]^{1/2}, \quad (32)$$

instead of Eq. (26).

Now we compare both results given by Eqs. (26) and (32) in the limit of $\xi = 0$ ($\Delta = 0$). In this limit, expressions in both Eqs. (15) and (30) go to unity. In the right-hand side of Eq. (26), the logarithmic divergence of $\ln(\xi_0/\xi)$ in the numerator is compensated by the divergence of $\ln(2/\xi)$ from $\bar{F}$ in the denominator. As a result, the phase transition from the superconducting state to the normal state occurs at a finite critical angular momentum $I_c - I_0$. On the other hand, $\bar{F}_n$ in Eq. (31) is finite in the limit of $\xi = 0$, while the numerator in Eq. (32) diverges due to $\ln(\xi_0/\xi)$. Thus, $I - I_0$ becomes infinity in the limit of $\xi = 0$, and no sharp phase transition occurs. The pairing gap keeps a very small but finite value, as is seen in Eq. (25) by replacing $\bar{F}$ by $\bar{F}_n$ and $\langle g\rangle_{\rm av}$ by $\langle g\rangle_n$. The finiteness of a nucleus assigns a measurable value to the average level distance d. As a result, the region with $\Delta < d/2$ covers a wide range of $I - I_0$.

In Figs. 6 and 7, we show the $I - I_0$ dependence of Δ and $\mathcal{J}_x$, respectively. These results are calculated from

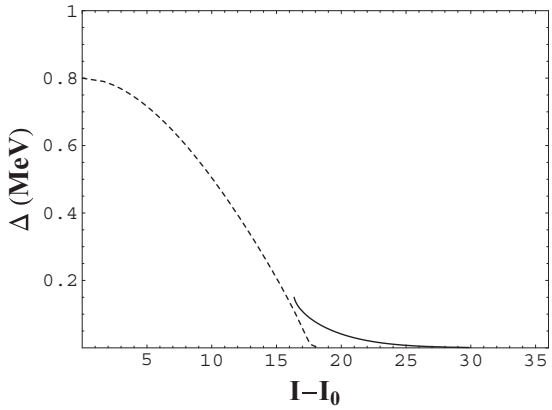

FIG. 6. The gap Δ as a function of the angular-momentum difference $I - I_0$ for an even-even nucleus. The dashed line is based on Eq. (25) with Eqs. (15) and (23), while the solid line is based on Eq. (25) with Eqs. (30) and (31). The starting gap parameter is $\Delta_0 = 0.8$ MeV at $I = I_0$, and the other parameters are given in the text.

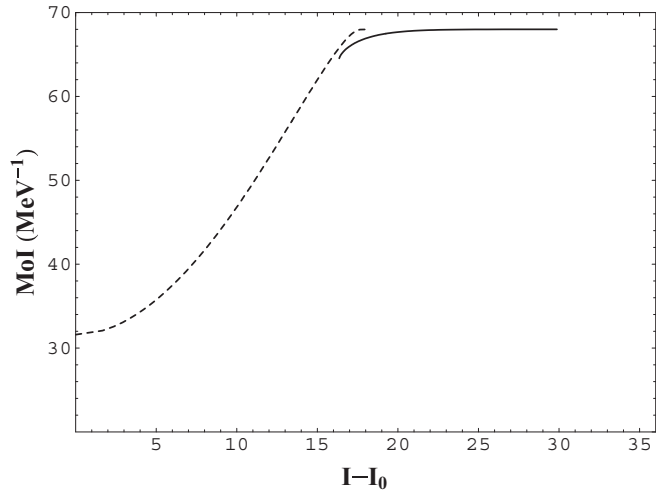

FIG. 7. The moment of inertia (MoI) $\mathcal{J}_x$ as a function of the angular-momentum difference $I - I_0$ for an even-even nucleus. The dashed line is based on Eq. (26), and the solid line on Eq. (32). The parameters are the same as those in Fig. 7.

Eqs. (26) (integral form) and (32) (sum form). We take a common parameter set of $\rho = 2.5\ {\rm MeV}^{-1}$, $\mathcal{J}_x^{\rm rig} = 68\ {\rm MeV}^{-1}$, $\delta = 2.0$ MeV, and $\xi_0 = 0.8$ in both calculations. As for the MoI, Eq. (26) is with Eq. (15) (integral form), and Eq. (32) with Eq. (30) (sum form). The starting value of ξ is 0.15 for Eq. (32) (sum form). The dashed line in Fig. 6 stands for the same curve displayed in a different way in Fig. 4. The dashed line shows the sharp phase transition around $I - I_0 \sim 18$, while the solid line does not indicate any phase transition within the range of $I - I_0 \lesssim 30$. Similarly, in Fig. 7, the dashed line shows a rapid increase of MoI, while the solid line shows a slow increase. In summary, the adoption of Γ_n and Z_n in Eqs. (30), (31), and (32) describes the slow decrease of Δ and the gradual increase of $\mathcal{J}_x$ over the high-spin region. As a result, the behavior of the MoI curve employing the expression in Eq. (30) becomes convex upward for large $I - I_0$, and it avoids a sharp phase transition to the rigid MoI at a certain finite critical I_c.

VI. INTEGRAL FORM AND SUM FORM FOR AN ODD-MASS NUCLEUS

We assume that a valence nucleon occupies a certain quasiparticle state labeled ℓ for the odd-mass case. Such a quasivacuum is given by $|\rangle\rangle \equiv \alpha_\ell^\dagger|\rangle$, where $|\rangle$ denotes the vacuum for the quasiparticle α_i or the vacuum for a neighboring even-even nucleus. We remark that $|\rangle\rangle$ is annihilated by $\alpha_i (i \neq \ell)$ and $\alpha_\ell^\dagger$. Minimizing the expectation value of H in Eq. (1) by the state $|\rangle\rangle$ under the constraints of Eq. (3) gives the CHFB equation for an odd-mass nucleus. The standard form of the CHFB equation (4) holds, provided that $A_{\ell\alpha}$ and $B_{\ell\alpha}$ are interchanged or Λ_ℓ is replaced by $-\Lambda_\ell$. Then, the CHFB equation takes a common expression as given by Eq. (4) for all the quasiparticle states including ℓth state.

As for the BCS solution when $\Omega_x = 0$, we have $E_{\bar{\ell}} = -E_\ell = \sqrt{(\varepsilon_\ell - \lambda)^2 + \Delta^2}$. Then, we can choose $u_\ell = u_{\bar{\ell}} = \sqrt{[1 + (\varepsilon_\ell - \lambda)/E_{\bar{\ell}}]/2}$ and $v_\ell = v_{\bar{\ell}} = \sqrt{[1 - (\varepsilon_\ell - \lambda)/E_{\bar{\ell}}]/2}$.

An application of the perturbation treatment similar to the case of the even-even nucleus yields the gap equation as

$$\Delta = \frac{G}{4}\sum_{\alpha\neq\ell,\tilde{\ell}}\frac{\Delta}{E_\alpha}\Bigg[1-\Omega_x^2\sum_{\beta\neq\ell,\tilde{\ell}}\frac{(j_x)^2_{\alpha\beta}}{E_\alpha+E_\beta}\left(\frac{E_\alpha E_\beta-(\varepsilon_\alpha-\lambda)(\varepsilon_\beta-\lambda)-\Delta^2}{E_\alpha E_\beta(E_\alpha+E_\beta)}+\frac{(\varepsilon_\alpha-\lambda)(\varepsilon_\alpha-\varepsilon_\beta)}{E_\alpha^2E_\beta}\right)$$
$$+\Omega_x^2\frac{(j_x)^2_{\alpha\ell}}{E_\alpha^2-E_{\tilde{\ell}}^2}\left(3-\frac{(\varepsilon_\alpha-\lambda)(\varepsilon_\ell-\lambda)+\Delta^2}{E_\alpha^2}\right)\Bigg]. \tag{33}$$

The third term in Eq. (33) works to prevent Δ decreasing, because the sign before Ω_x^2 is positive in contrast to the second term. Within the same approximation as adopted in Secs. II and III, the third term is efficient only for $\varepsilon_\alpha=\varepsilon_\ell\pm\delta$. We rewrite the right-hand side of Eq. (33) into the sum of the part similar to the even-even case [see Eq. (7)] and the residual part relevant to $E_{\tilde{\ell}}$:

$$\frac{4}{G}=-\frac{2}{E_{\tilde{\ell}}}+\sum_\alpha\frac{1}{E_\alpha}\Bigg[1-\Omega_x^2\sum_\beta\frac{(j_x)^2_{\alpha\beta}}{E_\alpha+E_\beta}\left(\frac{E_\alpha E_\beta-(\varepsilon_\alpha-\lambda)(\varepsilon_\beta-\lambda)-\Delta^2}{E_\alpha E_\beta(E_\alpha+E_\beta)}+\frac{(\varepsilon_\alpha-\lambda)(\varepsilon_\alpha-\varepsilon_\beta)}{E_\alpha^2E_\beta}\right)\Bigg]$$
$$-2\Omega_x^2\sum_{\alpha>0,\alpha\neq\ell}\frac{(j_x)^2_{\alpha\ell}}{E_{\tilde{\ell}}\left(E_{\tilde{\ell}}^2-E_\alpha^2\right)}\left[3-\frac{(\varepsilon_\alpha-\lambda)(\varepsilon_\ell-\lambda)+\Delta^2}{E_{\tilde{\ell}}^2}\right]. \tag{34}$$

The summations in the second term of this equation extend over all the states including ℓ and $\tilde{\ell}$, whose quasiparticle energies are expressed as positive quantities. The factor 2 in the first term comes from the degeneracy of ℓ and $\tilde{\ell}$ levels, and the sum $\sum_{\alpha>0,\alpha\neq\ell}$ excludes the time-reversed state $\tilde{\alpha}$.

From Eq. (8), the MoI is given in the first-order perturbation by

$$\mathcal{J}_x=\sum_{\varepsilon_\alpha<\varepsilon_\beta}\frac{(j_x)^2_{\alpha\beta}}{E_\alpha+E_\beta}\left(1-\frac{(\varepsilon_\alpha-\lambda)(\varepsilon_\beta-\lambda)+\Delta^2}{E_\alpha E_\beta}\right)$$
$$+2\sum_{\alpha>0,\alpha\neq\ell}\frac{(j_x)^2_{\alpha\ell}}{E_\alpha^2-E_{\tilde{\ell}}^2}\left(E_{\tilde{\ell}}+\frac{(\varepsilon_\alpha-\lambda)(\varepsilon_\ell-\lambda)+\Delta^2}{E_{\tilde{\ell}}}\right). \tag{35}$$

The second term is effective only for $\varepsilon_\alpha=\varepsilon_\ell\pm\delta$ and contributes to increase MoI. The second-order perturbation yields an additional contribution in the form of $\Omega_x(j_x)_{\alpha\beta}(j_x)_{\alpha\ell}(j_x)_{\beta\ell}$ ($\alpha,\beta\neq\ell,\tilde{\ell}$), but it can be disregarded within the present approximation scheme neglecting matrix elements between two states of α and β, whose energies are related by $\varepsilon_\alpha=\varepsilon_\beta\pm2\delta$ or $\varepsilon_\alpha=\varepsilon_\beta$.

The number constraint is given by

$$N=\frac{\varepsilon_\ell-\lambda}{E_{\tilde{\ell}}}+\sum_\alpha v_\alpha^2+\frac{\Omega_x^2}{2}\sum_{\alpha,\beta}\frac{(j_x)^2_{\alpha\beta}}{E_\alpha+E_\beta}\Bigg[\frac{\varepsilon_\alpha-\lambda}{E_\alpha(E_\alpha+E_\beta)}$$
$$\times\left(1-\frac{(\varepsilon_\alpha-\lambda)(\varepsilon_\beta-\lambda)+\Delta^2}{E_\alpha E_\beta}\right)-\frac{\Delta^2(\varepsilon_\alpha-\varepsilon_\beta)}{E_\alpha^3E_\beta}\Bigg]$$
$$+\frac{\Omega_x^2\Delta^2}{E_{\tilde{\ell}}^3}\sum_{\alpha>0,\alpha\neq\ell}\frac{(j_x)^2_{\alpha\ell}(\varepsilon_\alpha-\varepsilon_\ell)\left(5E_{\tilde{\ell}}^2-E_\alpha^2\right)}{\left(E_\alpha^2-E_{\tilde{\ell}}^2\right)^2}. \tag{36}$$

Here, the integer N is odd, and $N-1$ is even. These equations agree with those obtained in Ref. [19] except for the last term in Eq. (36), which was neglected in the latter numerical analysis.

We briefly consider the effect caused by the occupation of one nucleon in the ℓth orbital when $\Omega_x=0$, which is called the blocking effect. In such a case, Eqs. (33) and (36) are reduced to

$$\Delta=\frac{G}{4}\sum_{\alpha\neq\ell,\tilde{\ell}}\frac{\Delta}{E_\alpha},\quad N-1=\sum_{\alpha\neq\ell,\tilde{\ell}}v_\alpha^2. \tag{37}$$

On the other hand, when $\Omega_x=0$, Eqs. (7) and (27) are reduced to

$$\Delta^e=\frac{G}{4}\sum_\alpha\frac{\Delta^e}{E_\alpha^e},\quad N-1=\sum_\alpha\left(v_\alpha^e\right)^2, \tag{38}$$

where the superscript e denotes the even-even nucleus. We express small shifts due to the blocking effect as $\delta\Delta$ and $\delta\lambda$:

$$\Delta=\Delta^e+\delta\Delta,\quad \lambda=\lambda^e+\delta\lambda. \tag{39}$$

We expand two equations in Eq. (37) up to the first order in $\delta\Delta$ and $\delta\lambda$ and compare them with Eq. (38). The blocking effect is described by

$$\delta\Delta\cong-\frac{A(\Delta^e)^2/E_\ell^e-2B\left(v_\ell^e\right)^2}{\Delta^e((A\Delta^e)^2+B^2)},\quad \delta\lambda\cong\frac{B/E_\ell^e+2A\left(v_\ell^e\right)^2}{(A\Delta^e)^2+B^2}, \tag{40}$$

where

$$A\equiv\frac{1}{2}\sum_{\alpha\neq\ell,\tilde{\ell}}\frac{1}{\left(E_\alpha^e\right)^3},\quad B\equiv\frac{1}{2}\sum_{\alpha\neq\ell,\tilde{\ell}}\frac{\varepsilon_\alpha-\lambda^e}{\left(E_\alpha^e\right)^3}. \tag{41}$$

If we assume $\varepsilon_\ell\sim\lambda^e$ as was adopted by Nilsson and Prior [29], we have $B\cong0$ and

$$\delta\Delta=-\delta\lambda\cong-\frac{1}{A(\Delta^e)^2}. \tag{42}$$

Thus, the pairing gap for the odd-mass nucleus is smaller than the one for the even-even nucleus. Usually, $\delta\lambda$ is negligible in comparison with $|\lambda|$, because $|\lambda|$ is much larger than Δ.

While both Δ and λ at $\Omega_x=0$ differ from those in the even-even nucleus, a similar technique, which is developed in Secs. II and III, is applicable to the second term in the right-hand side of Eq. (34) and the first term in the right-hand side of Eq. (35), because all of them have the same forms as the even-even case. As for the factor $(j_x)^2_{\alpha\ell}$, we introduce two parameters: $j_>^2/4=(j_x)^2_{\alpha\ell}$ for $\varepsilon_\alpha>\varepsilon_\ell$ and $j_<^2/4$ for $\varepsilon_\alpha<\varepsilon_\ell$. Introducing another parameter, $\eta\equiv2(\varepsilon_\ell-\lambda)/\delta$, in analogy to

$\xi = 2\Delta/\delta$, we rewrite Eq. (35) as

$$\mathcal{J}_x = \mathcal{J}_x^{\rm rig}\left[1 - \xi^2 \ln\frac{1+\sqrt{1+\xi^2}}{\xi} + \frac{19}{90}\xi^2\right] + X_1\sqrt{\xi^2+\eta^2} + \frac{X_2}{\sqrt{\xi^2+\eta^2}}, \tag{43}$$

where

$$X_1 \equiv \frac{1}{2\delta}\left(\frac{j_>^2}{1+\eta} + \frac{j_<^2}{1-\eta}\right), \quad X_2 \equiv \frac{\eta}{2\delta}\left(\frac{j_>^2}{1+\eta} - \frac{j_<^2}{1-\eta}\right). \tag{44}$$

Only for a special case with $\varepsilon_\ell - \lambda = \delta/2$ and $\varepsilon_\alpha - \lambda = -\delta/2$ does $\eta = 1$ hold, and subsequently $E_\alpha = E_{\bar\ell}$. However, such a degenerate case is excluded by the assumption as mentioned below Eq. (6).

In the limit of $\xi = 0$, we get

$$\mathcal{J}_x^{\rm rig}({\rm odd}) - \mathcal{J}_x^{\rm rig}({\rm even}) = \frac{1}{2\delta}(j_>^2 - j_<^2). \tag{45}$$

This difference is 0.69 MeV^{-1} with the formula $A^{5/3}/72$ MeV^{-1} between A and $A+1$ for $A = 160 \sim 164$. If $j_>^2 = j_<^2$, $\mathcal{J}_x^{\rm rig}$(odd) coincides with $\mathcal{J}_x^{\rm rig}$(even). For simplicity, we fix $j_>^2 - j_<^2 = 2[\mathcal{J}_x^{\rm rig}({\rm odd}) - \mathcal{J}_x^{\rm rig}({\rm even}) \sim 0.5{\rm MeV}^{-1}]$, so that we can see the difference between even-even and odd-mass nuclei clearly.

Similarly, Eq. (34) becomes

$$\rho\delta\ln\left(\frac{\xi_0}{\xi}\right) = \frac{1}{\sqrt{\xi^2+\eta^2}} - \frac{1}{\sqrt{\xi_0^2+\eta^2}} + \frac{\Omega_x^2}{\delta}\left(\frac{\mathcal{J}_x^{\rm rig}\bar F}{8} - \frac{X_1}{\sqrt{\xi^2+\eta^2}} + \frac{X_2}{(\sqrt{\xi^2+\eta^2})^3}\right), \tag{46}$$

where $\bar F$ is defined in Eq. (23) and ξ_0 is the initial value of ξ in the odd-mass nucleus at $\Omega_x = 0$, which is smaller than the value in the even-even nucleus due to the blocking effect as inferred from Eqs. (40) and (42).

As for Eq. (36), the first and the second terms are derived without rotation, and the shifts of $\delta\Delta$ and $\delta\lambda$ are already included in the starting values of ξ_0 and λ in the odd-mass system. The third term does not affect λ at $\Omega_x \neq 0$ as is seen in Fig. 5. The last term in Eq. (36) is rewritten with $j_>^2$, $j_<^2$, and X_2 in Eq. (44) as

$$\frac{\Omega_x^2\xi^2}{2\delta^2}\left[\frac{1}{\sqrt{\xi^2+\eta^2}}\left(\frac{j_>^2}{(1+\eta)^2} - \frac{j_<^2}{(1-\eta)^2}\right) - \frac{2\delta X_2}{\eta(\sqrt{\xi^2+\eta^2})^3}\right]. \tag{47}$$

If we assume $j_>^2 = j_<^2$, which gives a common rigid-body value for both the even-even nucleus and the odd-mass nucleus, Eq. (47) is reduced to

$$\Omega_x^2\left(\frac{\xi}{\delta}\right)^2 \frac{j_>^2\eta(1-3\eta^2)}{(\xi^2+\eta^2)^{3/2}(1-\eta^2)^2}, \tag{48}$$

as long as the contribution from ξ^4 is neglected. The quantity given by Eq. (48) vanishes for $\xi = 0$ (large angular-momentum region) and $\eta = 0$, i.e., the blocking effect as studied by Nilsson and Prior [29], or $\eta^2 = 1/3$. We can neglect the change in λ by rotation as long as we choose $\eta^2 \sim 1/3$.

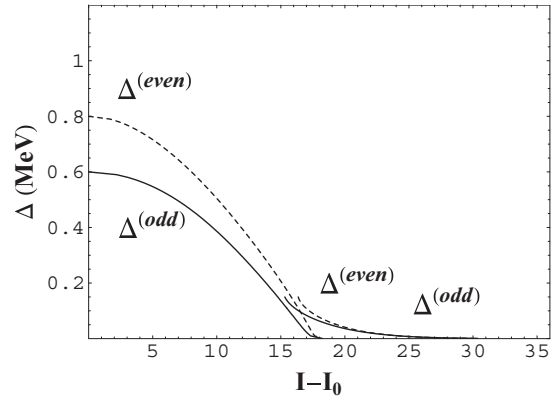

FIG. 8. Comparison of gap Δ between the even-even case ($\Delta^{(\rm even)}$ with dashed line) and the odd-mass case ($\Delta^{(\rm odd)}$ with solid line). The parameters for the odd-mass case are $j_>^2 = 12$, $j_<^2 = 10$, $\xi_0 = 0.6$, and $\eta = 0.6$. Lines for the even-even case are the same as those in Fig. 6.

As for the matrix element $(j_x)^2_{\alpha\ell}$, we consult with the one for the orbital angular momentum given in Ref. [15]:

$$\langle Nn_z'\Lambda \pm 1|\ell_x \pm i\ell_y|Nn_z\Lambda\rangle = \frac{\omega_z+\omega_\perp}{2\sqrt{\omega_z\omega_\perp}}\left[\sqrt{(n_z+1)(N-n_z\mp\Lambda)}\delta_{n_z' n_z+1} + \sqrt{n_z(N-n_z\pm\Lambda+2)}\delta_{n_z' n_z-1}\right]. \tag{49}$$

We approximate the coefficient before $[\cdots]$ to be almost one and neglect the contribution from the spin part to the matrix element of $(j_x)^2_{\alpha\ell}$. Then, if we assume the level ℓ is [521]3/2, $j_>^2 = 12$ for the transition to [512]5/2 and $j_<^2 = 12$ for the transition to [530]1/2. If the level ℓ is [532]3/2, $j_>^2 = 18$ to [523]5/2 and $j_<^2 = 16$ to [541]1/2. If the level ℓ is [512]5/2, $j_>^2 = 8$ to [503]7/2 and $j_<^2 = 4$ to [523]7/2. We adopt $j_>^2 = 12$ and $j_<^2 = 10$ in Figs. 8, 9, 10, and 12.

From Eq. (46), we get the integral form for the odd-mass case as

$$(I-I_0)^2 = \delta^2\mathcal{J}_x^2\rho\left(\ln\frac{\xi_0}{\xi} - \frac{1}{\rho\delta\sqrt{\xi^2+\eta^2}} + \frac{1}{\rho\delta\sqrt{\xi_0^2+\eta^2}}\right) \times\left(\frac{\mathcal{J}_x^{\rm rig}\bar F}{8} - \frac{X_1}{\sqrt{\xi^2+\eta^2}} + \frac{X_2}{(\sqrt{\xi^2+\eta^2})^3}\right)^{-1}. \tag{50}$$

When $\Delta \ll 1/\rho$, we apply the same prescription as developed in Sec. V (sum form). We replace $\bar F$ in Eq. (50) by $\bar F_n$ in Eq. (31) to obtain

$$(I-I_0)^2 = \delta^2\mathcal{J}_x^2\rho\left(\ln\frac{\xi_0}{\xi} - \frac{1}{\rho\delta\sqrt{\xi^2+\eta^2}} + \frac{1}{\rho\delta\sqrt{\xi_0^2+\eta^2}}\right) \times\left(\frac{\mathcal{J}_x^{\rm rig}\bar F_n}{8} - \frac{X_1}{\sqrt{\xi^2+\eta^2}} + \frac{X_2}{(\sqrt{\xi^2+\eta^2})^3}\right)^{-1}. \tag{51}$$

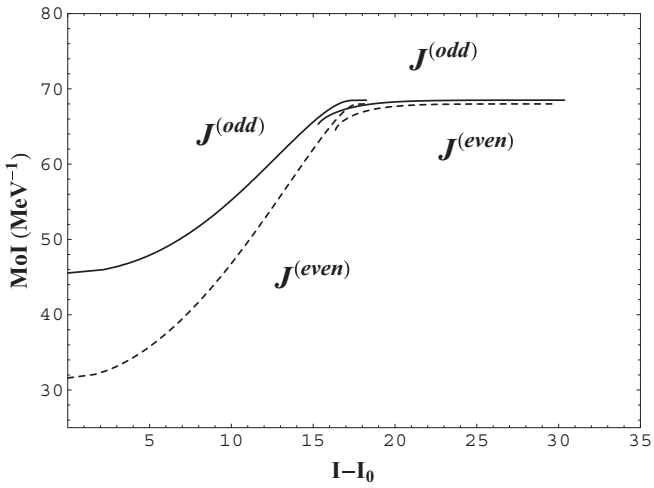

FIG. 9. Comparison of the MoI between the even-even case (dashed line) and the odd-mass case (solid line). The parameters are the same as those in Fig. 8.

In Eq. (43) we replace $\ln[(1+\sqrt{1+\xi^2})/\xi]$ by $\Gamma_n - \xi^2 Z_n$ to obtain

$$\mathcal{J}_x = \mathcal{J}_x^{\rm rig}\left[1-\xi^2\left(\Gamma_n - \xi^2 Z_n - \frac{19}{90}\right)\right] + X_1\sqrt{\xi^2+\eta^2} + \frac{X_2}{\sqrt{\xi^2+\eta^2}}. \quad (52)$$

VII. COMPARISON OF MOMENT OF INERTIA BETWEEN EVEN-EVEN AND ODD-MASS NUCLEI

In Fig. 8 we compare the gap values given by Eqs. (50) (integral form) and (51) (sum form) (solid lines with $\Delta^{(\rm odd)}$) with those for the even-even case (dashed lines with $\Delta^{(\rm even)}$), which are the same as those in Fig. 6. The parameters for the odd-mass case are $\eta = 0.6$, $\xi_0 = 0.6$, $j_>^2 = 12$, and $j_<^2 = 10$. The other parameters are common for both even-even and odd-mass cases, i.e., $\delta = 2.0$ MeV, $\mathcal{J}_x^{\rm rig} = 68$ MeV^{-1}, and $\rho = 2.5$ MeV^{-1}. The gap for the odd-mass case starts from $\xi_0 = 0.6$, which is smaller than 0.8 for the even-even case due to the blocking effect. The value of $\eta = 0.6$ corresponds to $\eta^2 \sim 1/3$, and we have numerically confirmed that the quantity in Eq. (48) becomes vanishingly small (at most 0.0019) over all the region of ξ for this parameter set. We find that the decrease of $\Delta^{(\rm odd)}$ is more gradual, and the shape of the curve becomes convex downward in the asymptotic region. Comparing the right-hand side of Eq. (46) at $\xi = \xi_0$ with $1/(G\rho)$ for $G = 0.14$ MeV [28], we find that the applicability of the original perturbation expansion is limited to $I < 30$.

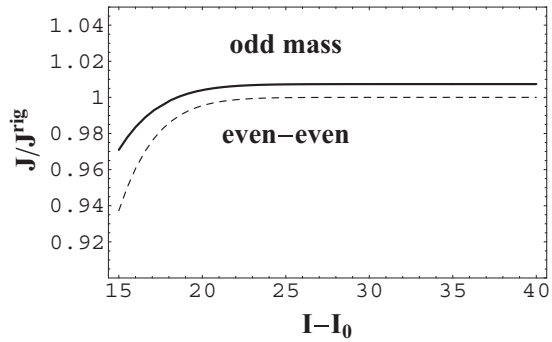

FIG. 10. Comparison of $\mathcal{J}_x/\mathcal{J}_x^{\rm rig}$ in the approximate sum form between the even-even case (dashed line) and the odd-mass case (solid line) in the high-spin region. In both cases, the parameters are the same as those in Figs. 8 and 9.

In Fig. 9, the MoI based on Eqs. (43) (integral form) and (52) (sum form) for the odd-mass case (solid lines with $J^{(\rm odd)}$) is compared with the MoI for the even-even case (dashed lines with $J^{(\rm even)}$), which is already shown in Fig. 7. Because of the blocking effect, $J^{(\rm odd)}$ starting from a value larger than $J^{(\rm even)}$ increases gradually and approaches the rigid-body value at large $I - I_0$.

Similar to the even-even case, the curve of $J^{(\rm odd)}$ is convex upward and approaches $\mathcal{J}_x^{\rm rig}$. The necessity of such behavior of the MoI has been confirmed by reproducing the experimental data of $E^* - aI(I+1)$ for TSD bands [2–4] (e.g., Fig. 10 in Ref. [4]). This trend is clearly seen in numerical results based on both Eq. (50) with $\bar{F}$ and Eq. (51) with $\bar{F}_n$.

To derive an analytic expression for both $\mathcal{J}^{(\rm even)}$ and $\mathcal{J}^{(\rm odd)}$ in the high-spin region where ξ is small enough, we neglect the ξ^2 and ξ^4 terms in the expressions with sum form, i.e., Eqs. (30), (32), (51), and (52). Thus, for the even-even case, Eq. (32) gives

$$\xi = \xi_0 e^{-P_e(I-I_0)^2}, \quad \text{with} \quad P_e \equiv \frac{2\Gamma_n - 371/360}{\delta^2\rho\mathcal{J}_x^{\rm rig}}. \quad (53)$$

Inserting this expression for ξ into Eq. (30) without the ξ^4 term, we get

$$\frac{\mathcal{J}_x}{\mathcal{J}_x^{\rm rig}} = 1 - \xi_0^2 Q_e e^{-2P_e(I-I_0)^2}, \text{ with } Q_e \equiv \Gamma_n - \frac{19}{90}. \quad (54)$$

In the plot of $\mathcal{J}_x/\mathcal{J}_x^{\rm rig}$ for the even-even case (dashed line in Fig. 10), we take $\xi_0 = 0.8$ for the initial value of ξ at $\Omega_x = 0$ ($I = I_0$).

Similarly, for the odd-mass case, assuming that ξ is much smaller than $\eta(=0.6)$ in Eqs. (51) and (52), we get the following from Eq. (51):

$$\begin{aligned} \xi &= \xi_0 e^{-R_1 - P_o(I-I_0)^2}, \\ \text{with} \quad R_1 &\equiv \frac{1}{\rho\delta}\left(\frac{1}{\eta} - \frac{1}{\sqrt{\xi_0^2+\eta^2}}\right), \\ P_o &\equiv \frac{P_e + P_1}{R_2^2}, \quad R_2 \equiv 1 + \frac{j_>^2 - j_<^2}{2\delta\mathcal{J}_x^{\rm rig}}, \\ \text{and} \quad P_1 &\equiv \frac{1}{2\delta\rho\left(\delta\eta\mathcal{J}_x^{\rm rig}\right)^2}\left(\frac{1-\eta}{1+\eta}j_>^2 - \frac{1+\eta}{1-\eta}j_<^2\right). \end{aligned} \quad (55)$$

We insert this approximate ξ into Eq. (52) without the ξ^4 term to obtain

$$\frac{\mathcal{J}_x}{\mathcal{J}_x^{\rm rig}} = R_2 - \xi_0^2\left(Q_e + \frac{1}{2}P_1\mathcal{J}_x^{\rm rig}\delta^2\rho\right)e^{-2R_1 - 2P_o(I-I_0)^2}. \quad (56)$$

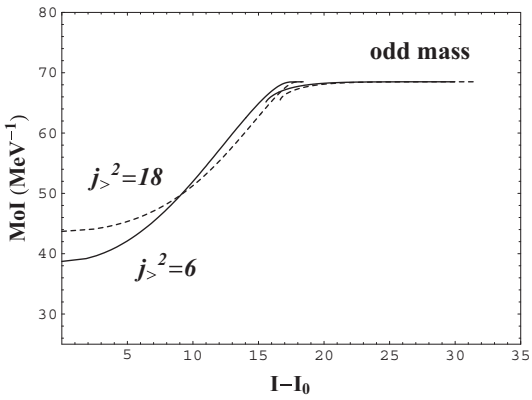

FIG. 11. Comparison of the MoI between two cases with $j_>^2 = 18$ (dashed line) and $j_>^2 = 6$ (solid line) for the odd-mass nucleus. In both cases, the other parameters are common, i.e., $j_<^2 = j_>^2 - 2$, $\xi_0 = 0.7$, and $\eta = 0.6$.

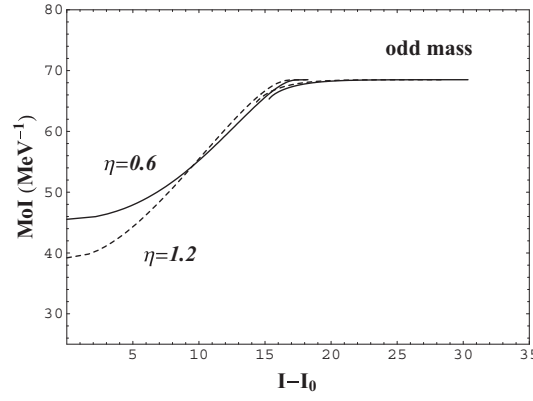

FIG. 12. Comparison of the MoI for different η values in the odd-mass nucleus as functions of $I - I_0$. The solid line corresponds to $\eta = 0.6$ and the dashed line to $\eta = 1.2$. The other parameters are common in both cases, i.e., $\xi_0 = 0.6$, $j_>^2 = 12$, and $j_<^2 = 10$.

In the plot of $\mathcal{J}_x/\mathcal{J}_x^{\rm rig}$ for the odd-mass case (solid line in Fig. 10), we take $\xi_0 = 0.6$ for the initial value of ξ at $\Omega_x = 0$ ($I = I_0$). Both the approximate solutions given by Eqs. (54) and Eq. (56) are compared in Fig. 10. The main difference between those comes from the initial value ξ_0^2, which includes the blocking effect. Both lines show convex upward before they reach to rigid-body values.

To study the effect of $j_>^2$, we compare two cases of $j_>^2 = 18$ and $j_>^2 = 6$ in Fig. 11 with the parameter set of $\xi_0 = 0.7$ and $\eta = 0.6$. Through the present analysis, we choose $j_<^2 = j_>^2 - 2$. As seen in Fig. 11, the blocking effect is larger for the larger $j_>^2$, even though ξ_0 is common. The blocking effect on the MoI depends on X_1 and X_2 in Eq. (44). When $\eta < 1$, X_1 is positive and larger than X_2. The critical angular momentum predicted by the integral form ($\xi = 0$) is larger for larger $j_>^2$ by about 2 units in $I - I_0$. If η is larger than 1, X_1 becomes negative. Then the blocking effect at $I = I_0$ becomes larger and the critical angular momentum becomes larger for the smaller $j_>^2$.

To study the effect of η, we compare $\eta = 0.6$ with $\eta = 1.2$ in Fig. 12. Because X_1 is negative for $\eta = 1.2$, the blocking effect is smaller. As for the effect on the chemical potential, Eq. (48) gives 0.036 at its maximum for $\eta = 1.2$, which is still in a negligible order.

If we suppose the last nucleons occupy ℓ_1 and ℓ_2 levels for the excited bands in the even-even nucleus or the valence levels in the odd-odd nucleus, then the summation in Eq. (33) should be replaced by $\sum_{\alpha\neq\ell_1,\ell_2,\tilde{\ell}_1,\tilde{\ell}_2}$. For example, the gap equation, Eq. (33), is replaced by

$$\Delta = \frac{G}{4}\sum_{\alpha\neq\ell_1,\ell_2,\tilde{\ell}_1,\tilde{\ell}_2}\frac{\Delta}{E_\alpha}\Bigg\{1-\Omega_x^2\sum_{\beta\neq\ell_1,\ell_2,\tilde{\ell}_1,\tilde{\ell}_2}\frac{(j_x)_{\alpha\beta}^2}{E_\alpha+E_\beta}\left(\frac{E_\alpha E_\beta-(\varepsilon_\alpha-\lambda)(\varepsilon_\beta-\lambda)-\Delta^2}{E_\alpha E_\beta(E_\alpha+E_\beta)}+\frac{(\varepsilon_\alpha-\lambda)(\varepsilon_\alpha-\varepsilon_\beta)}{E_\alpha^2 E_\beta}\right)$$
$$+\Omega_x^2\left[\frac{(j_x)_{\alpha\ell_1}^2}{E_\alpha^2-E_{\tilde{\ell}_1}^2}\left(3-\frac{(\varepsilon_\alpha-\lambda)(\varepsilon_{\ell_1}-\lambda)+\Delta^2}{E_\alpha^2}\right)+\frac{(j_x)_{\alpha\ell_2}^2}{E_\alpha^2-E_{\tilde{\ell}_2}^2}\left(3-\frac{(\varepsilon_\alpha-\lambda)(\varepsilon_{\ell_2}-\lambda)+\Delta^2}{E_\alpha^2}\right)\right]\Bigg\}. \quad (57)$$

This equation indicates that the existence of two blocked levels labeled ℓ_1 and ℓ_2 inducesa larger reduction of Δ (blocking effect [30,31]) and a slower decrease of Δ with increasing I (CAP effect) than the case with only one blocked level. In more detail, (i) when $\Omega_x = 0$, the sum in the first term extends over fewer numbers of levels, so that the blocking effect is more effective. (ii) As for the CAP effect caused by the terms with $\Omega_x(\neq 0)$, the contribution from the second term is reduced since the sum covers fewer numbers of levels, and the contribution from the third term with opposite sign increases because the sum covers a larger number of blocked levels. As a result, it is expected that Δ starts from a reduced value and its reduction rate with increasing I becomes smaller than that of the single blocked case.

VIII. CONCLUSION

We have applied the approximation method developed by Bohr and Mottelson [15] and by Bengtsson and Helgessen [16] to the CAP effect [17]. Using the second-order perturbed CHFB equation, we have derived the angular-momentum dependence of the MoI and of the gap parameter Δ for both even-even and odd-mass nuclei.

To solve the gap equation, we have applied alternative methods depending on the magnitude of the gap value. We have shown that in the region $\Delta \geqslant d/2$, both the MoI and the angular momentum I are related to $\xi(= 2\Delta/d)$ by integral forms, while in the region of $\Delta \ll d/2$, both are expressed by sum forms. As a result, the MoI is expressed as an analytic

function of I mediated by the parameter ξ. We found that MoI continuously increases with increasing I and its functional behavior is convex upward till it approaches the rigid-body value, while the gap parameter slowly decreases and follows a curve convex downward till it approaches zero asymptotically. Subsequently, the phase transition from super state to normal state never occurs due to the finiteness of a nucleus.

For the odd-mass nucleus, we have discussed the effect of the level occupied by one valence nucleon and relevant matrix elements. The blocking effect reduces the starting value of Δ and increases that of the MoI. Therefore, the behavior of the MoI in the odd-mass nucleus shows a more gradual increase as a function of I compared with that of the even-even nucleus. Needless to say, such a slow increase of the MoI with increasing I is consistent with the conclusion assessed from the analysis by applying the particle-rotor model to the TSD bands [2–4].

Neglecting higher-order terms in ξ within the sum forms, we directly express the MoI as analytic functions of $I - I_0$ in Eqs. (54) and (56).

Finally, we remark that the centrifugal stretching effect on the MoI will be included by the third-order perturbation in the expectation value of $\hat{I}_x$ within the present scheme.

ACKNOWLEDGMENTS

The authors express their sincere thanks to Dr. A. O. Macchiavelli for turning their attention to the lecture note by D. Bengtsson and J. Helgesson [16].

APPENDIX A: APPROXIMATION FOR THE INTEGRAND $g(x)$

For a technical purpose, first we rewrite the integral of the function $g(x)$, which is symmetric about $x = -\delta/2$, as

$$\int_{-3\delta/2}^{\delta/2} g(x)dx = \int_{-\delta/2}^{\delta/2} [g(x) + g(x-\delta)]dx = 2\int_{-\delta/2}^{0} [g(x) + g(x-\delta)]dx. \quad \text{(A1)}$$

As directly confirmed from the expression in Eq. (14), $g(x) + g(x-\delta)$ is an even function of x and is symmetric about $x = 0$. Regarding x/δ, $\sqrt{x^2+\Delta^2}/\delta$, and Δ/δ as equally small quantities, we expand $g(x) + g(x-\delta)$ up to the second order in these quantities. Then, we get

$$g(x) + g(x-\delta) \cong 1 - \frac{\delta}{2}\frac{\xi^2}{\sqrt{x^2+\Delta^2}} + \frac{3}{8}\xi^2, \quad \text{(A2)}$$

where ξ is defined by Eq. (10). In Fig. 13, we compare the original function $g(x) + g(x-\delta)$, which is labeled "exact," with the approximate expression labeled "approx.," which is given by the right-hand side of Eq. (A2), in the range $-\delta/2 \leqslant x \leqslant \delta/2$ for the case of $\xi = 0.2$. Both agree at $x = 0$, but there remains a discrepancy by $-(59/72)\xi^2$ at $x/\delta = \pm 1/2$. Because we have included up to the second order in x/δ, we assume such a difference comes from the fourth-order contribution $(x/\delta)^4$, whose coefficient is determined from the difference at $x/\delta = \pm 1/2$ between the quantity approximated by Eq. (A2) and the one estimated with the original expression in Eq. (14). Taking account of this difference, we propose an expression for an actual use in the text:

$$g(x) + g(x-\delta) \cong 1 - \frac{\delta}{2}\frac{\xi^2}{\sqrt{x^2+\Delta^2}} + \frac{3}{8}\xi^2 - \frac{118\xi^2}{9}\left(\frac{x}{\delta}\right)^4. \quad \text{(A3)}$$

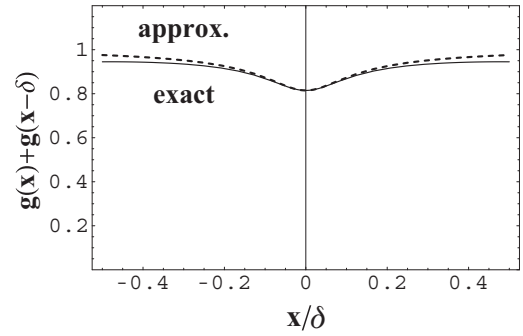

FIG. 13. Difference between the function $g(x) + g(x-\delta)$ given by Eq. (14) (exact) and the approximate one given by Eq. (A2) (approx.) within the interval $-\delta/2 \leqslant x = \varepsilon_\alpha - \lambda \leqslant \delta/2$.

APPENDIX B: APPROXIMATION FOR THE INTEGRAND $f(x)$

To integrate $f(x)$, we introduce the summed function of $F(x) \equiv f(x) + f(x-\delta)$, which is an even function of x, and limit the interval of the integral to $-\delta/2 \leqslant x \leqslant \delta/2$:

$$\int_{-3\delta/2}^{\delta/2} f(x)dx = \int_{-\delta/2}^{\delta/2} [f(x) + f(x-\delta)]dx = 2\int_{-\delta/2}^{0} F(x)dx. \quad \text{(B1)}$$

The behavior of $F(x)$ for the case of $\Delta = 0.1$ MeV and $\delta = 1$ MeV is shown by the solid line in Fig. 14. The peaks in $F(x)$ are located around $x = \pm\Delta$. To perform the integral without destroying the functional dependence on Δ or ξ, we proceed with an analytic integration as follows: Regarding

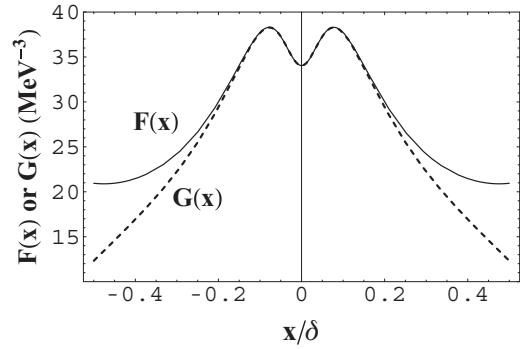

FIG. 14. Comparison between the functions $F(x)$ and $G(x)$ as functions of $x(= \varepsilon_\alpha - \lambda)$ for the case of $\Delta = 0.1$ MeV and $\delta = 1$ MeV.

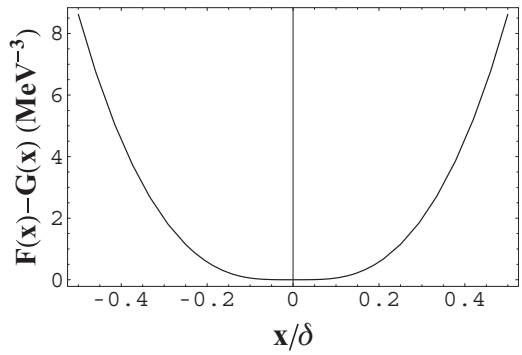

FIG. 15. Difference $F(x) - G(x)$ as a function of $x(= \varepsilon_\alpha - \lambda)$ for the case of $\Delta = 0.1$ MeV and $\delta = 1$ MeV.

x/δ, $\sqrt{x^2+\Delta^2}/\delta$, and Δ/δ as equally small quantities, we expand $F(x)$ around $x = 0$ up to the second order in those quantities and name it as $G(x)$:

$$\begin{aligned} F(x) &\cong \frac{2}{\delta^3}\left\{\frac{4\delta}{\sqrt{x^2+\Delta^2}}\left[1-6\left(\frac{\Delta}{\delta}\right)^2\right]-3\right. \\ &\quad +16\frac{\sqrt{x^2+\Delta^2}}{\delta}-25\frac{x^2}{\delta^2}+\frac{5}{2}\left(\frac{\Delta}{\delta}\right)^2 \\ &\quad \left.-\frac{2\delta^3}{(\sqrt{x^2+\Delta^2})^3}\left(\frac{\Delta}{\delta}\right)^2\left[1-4\left(\frac{\Delta}{\delta}\right)^2\right]\right\} \\ &\equiv G(x). \end{aligned} \tag{B2}$$

The behavior of the approximate function $G(x)$ is also shown in Fig. 14 by the dashed line, which simulates $F(x)$ very well, except for the region close to $x/\delta = \pm 1/2$. The difference between $F(x)$ and $G(x)$ is shown in Fig. 15. Because $G(x)$ takes into account up to the order of x^2, we assume that the remaining part of $F(x) - G(x)$ comes from the contribution of x^4. The coefficient for x^4 at $x/\delta = \pm 1/2$ is given by $[F(\pm\delta/2) - G(\pm\delta/2)](2/\delta)^4$. We integrate $G(x)$ analytically and add two areas below the curve $F(x) - G(x)$ as shown in Fig. 15. Finally, we arrive at an analytic form of the integral up to the second order in ξ:

$$\begin{aligned} \int_{-3\delta/2}^{\delta/2} f(x)dx &= 2\int_{-\delta/2}^{0} F(x)dx \\ &\cong 2\int_{-\delta/2}^{0} G(x)dx + \frac{\delta}{5}\left[F\left(-\frac{\delta}{2}\right)-G\left(-\frac{\delta}{2}\right)\right] \\ &= \frac{1}{\delta^2}\left[16(1-\xi^2)\ln\left(\frac{1+\sqrt{1+\xi^2}}{\xi}\right)\right. \\ &\quad \left.+\frac{319}{27}\xi^2-\frac{371}{45}\right] \\ &\equiv \frac{\bar{F}}{\delta^2}. \end{aligned} \tag{B3}$$

In the text, we make use of the dimensionless quantity $\bar{F}$, which is a function of ξ only.

APPENDIX C: APPLICATION OF ASYMPTOTIC SERIES EXPANSION TO THE CRITICAL REGION OF $\Delta \ll d/2$

If $2\Delta/d$ is small enough, the right-hand side of Eq. (29) can be well approximated by the expansion retaining up to its second-order term:

$$\begin{aligned} &\sum_{x>0}^{\delta/2}\frac{1}{\sqrt{x^2+\Delta^2}} \\ &\quad \cong \frac{2}{d}\left[\sum_{i=1}^{n}\frac{1}{2i-1}-\frac{1}{2}\left(\frac{2\Delta}{d}\right)^2\sum_{i=1}^{n}\frac{1}{(2i-1)^3}\right]. \end{aligned} \tag{C1}$$

Making use of the following identities,

$$\sum_{i=1}^{n}\frac{1}{(2i-1)^k} = \sum_{i=1}^{2n}\frac{1}{i^k}-\frac{1}{2^k}\sum_{i=1}^{n}\frac{1}{i^k}, \tag{C2}$$

for $k = 1$ and 3, we rewrite Eq. (C1) as

$$\sum_{x>0}^{\delta/2}\frac{1}{\sqrt{x^2+\Delta^2}} \cong \frac{2}{d}\left[\sum_{i=1}^{2n}\frac{1}{i}-\frac{1}{2}\sum_{i=1}^{n}\frac{1}{i}-\frac{1}{2}\left(\frac{2\Delta}{d}\right)^2\left(\sum_{i=1}^{2n}\frac{1}{i^3}-\frac{1}{2^3}\sum_{i=1}^{n}\frac{1}{i^3}\right)\right]. \tag{C3}$$

To each of four sums, we apply the asymptotic series expansions [32]:

$$\sum_{i=1}^{n}\frac{1}{i} = \gamma + \ln n + \frac{1}{2n} - \frac{1}{12n(n+1)} - \frac{1}{12n(n+1)(n+2)} - \cdots \tag{C4}$$

and

$$\sum_{i=1}^{n}\frac{1}{i^k} = \zeta(k) - \frac{1}{2(n+1)^k} - \frac{1}{(k-1)(n+1)^{k-1}} - \cdots, \quad (k \geqslant 2), \tag{C5}$$

where γ $(= 0.577\ldots)$ is the Euler constant, and $\zeta(k)$ the Riemann ζ function.

Thus, Eq. (C3) is rewritten as

$$\sum_{x>0}^{\delta/2}\frac{1}{\sqrt{x^2+\Delta^2}} \cong \frac{1}{d}(\Gamma_n - \xi^2 Z_n), \tag{C6}$$

with

$$\Gamma_n \equiv \gamma + \ln 4n + \frac{1}{12n}\left[\frac{1}{n+1} - \frac{1}{2n+1} + \frac{1}{(n+1)(n+2)} - \frac{1}{2(n+1)(2n+1)}\right] + \cdots$$
$$\cong \gamma + \ln 4n \tag{C7}$$

and

$$Z_n \equiv \left(\frac{\delta}{d}\right)^2\left[\frac{7}{8}\zeta(3) + \frac{1}{16}\left(\frac{1}{(n+1)^3} + \frac{1}{(n+1)^2}\right) - \frac{1}{2}\left(\frac{1}{(2n+1)^3} + \frac{1}{(2n+1)^2}\right) + \cdots\right]$$
$$\cong \left(\frac{\delta}{d}\right)^2\frac{7}{8}\zeta(3), \tag{C8}$$

where $\zeta(3) = 1.202\ldots$ [33]. Regarding n being large enough, we have retained only leading terms in Γ_n and Z_n. We confirm that neglected contributions in Eqs. (C7) and (C8) are small enough even for $n = 3$.

[1] K. Tanabe and K. Sugawara-Tanabe, Phys. Rev. C **73**, 034305 (2006); **75**, 059903(E) (2007).
[2] K. Tanabe and K. Sugawara-Tanabe, Phys. Rev. C **77**, 064318 (2008).
[3] K. Sugawara-Tanabe and K. Tanabe, Phys. Rev. C **82**, 051303(R) (2010).
[4] K. Sugawara-Tanabe, K. Tanabe, and N. Yoshinaga, Prog. Theor. Exp. Phys. **2014**, 063D01 (2014).
[5] S. W. Ødegård *et al.*, Phys. Rev. Lett. **86**, 5866 (2001).
[6] D. R. Jensen *et al.*, Phys. Rev. Lett. **89**, 142503 (2002).
[7] D. R. Jensen *et al.*, Nucl. Phys. A **703**, 3 (2002).
[8] G. Schönwaßer *et al.*, Phys. Lett. B **552**, 9 (2003).
[9] H. Amro *et al.*, Phys. Lett. B **553**, 197 (2003).
[10] A. Görgen *et al.*, Phys. Rev. C **69**, 031301(R) (2004).
[11] P. Bringel *et al.*, Phys. Rev. C **73**, 054314 (2006).
[12] G. B. Hagemann, Eur. Phys. J. A **20**, 183 (2003).
[13] D. J. Hartley *et al.*, Phys. Rev. C **80**, 041304(R) (2009).
[14] P. Bringel *et al.*, Phys. Rev. C **75**, 044306 (2007).
[15] A. Bohr and B. R. Mottelson, *Nuclear Structure* (Benjamin, MA, 1975), Vol. II, p. 82.
[16] D. Bengtsson and J. Helgessen, lecture notes from a summer school at Oak Ridge, 1991 (unpublished).
[17] B. R. Mottelson and J. G. Valatin, Phys. Rev. Lett. **5**, 511 (1960).
[18] M. Sano and M. Wakai, Nucl. Phys. **67**, 481 (1965).
[19] K. Sugawara, Prog. Theor. Phys. **35**, 44 (1966).
[20] B. Banerjee, H. J. Mang, and P. Ring, Nucl. Phys. A **215**, 366 (1973).
[21] N. Pietralla and O. M. Gorbachenko, Phys. Rev. C **70**, 011304(R) (2004); A. Costin *et al.*, *ibid.* **79**, 024307 (2009); M. K. Smith *et al.*, *ibid.* **87**, 044317 (2013).
[22] K. Tanabe and K. Sugawara-Tanabe, Phys. Lett. B **135**, 353 (1984); Prog. Theor. Phys. **83**, 1148 (1990); Phys. Lett. B **259**, 12 (1991).
[23] J. L. Egido, P. Ring, S. Iwasaki, and H. J. Mang, Phys. Lett. B **154**, 1 (1985).
[24] Y. Sun and J. L. Egido, Phys. Rev. C **50**, 1893 (1994).
[25] D. R. Inglis, Phys. Rev. **96**, 1059 (1954).
[26] A. B. Migdal, Nucl. Phys. **13**, 655 (1959).
[27] R. B. Firestone and V. S. Stirley, *Table of Isotopes* (Wiley & Sons, New York, 1996), Vol. II, p. H-6.
[28] A. Bohr and B. R. Mottelson, *Nuclear Structure* (Benjamin, MA, 1975), Vol. II, p. 652.
[29] S. G. Nilsson and O. Prior, Mat. Fys. Medd. K. Dan. Vidensk. Selsk. **32**, no. 16, 3 (1961).
[30] A. Odahara, Y. Gono, T. Fukuchi, Y. Wakabayashi, H. Sagawa, W. Satuła, and W. Nazarewicz, Phys. Rev. C **72**, 061303(R) (2005).
[31] J. Rissanen, R. M. Clark, A. O. Macchiavelli, P. Fallon, C. M. Campbell, and A. Wiens, Phys. Rev. C **90**, 044324 (2014).
[32] S. Moriguti, K. Udagawa, and S. Hitotumatu, *Sugaku Koushiki* (Mathematical Formulas) (Iwanami Shoten, Publishers, Tokyo, 1957), Vol. II, p. 7.
[33] S. Moriguti, K. Udagawa, and S. Hitotumatu, *Sugaku Koushiki* (Mathematical Formulas) (Iwanami Shoten, Publishers, Tokyo, 1957), Vol. II, p. 39.